23rd ABCM International Congress of Mechanical Engineering
December 6-11, 2015, Rio de Janeiro, RJ, Brazil

ANALYSIS OF THE INFLUENCE OF INTRODUCTION OF THE STABILIZER BAR ON VEHICLE DYNAMIC

Wagner Barth Lenz
UTFPR-PG, Ponta Grossa, Brazil
wagner_barth@hotmail.com

Angelo Marcelo Tusset
UTFPR-PG, Ponta Grossa, Brazil
tusset@utfpr.edu.br

Vinícius Piccirillo
UTFPR-PG, Ponta Grossa, Brazil
piccirillo@utfpr.edu.br

Frederic Conrad Janzen
Universidade Tecnológica Federal do Paraná
fcjanzen@utfpr.edu.br

José Manoel Balthazar
UNESP-ITA, Bauru-São José dos Campos, Brazil
jmbaltha@gmail.com

Abstract. *This paper proposes the introduction of a stabilizing bar in a full-car model with nonlinear suspension. The majority of mathematical models proposed in the literature ignore the influence of the stabilizer bar, in the vehicle dynamics. The analysis of the influence of the addition of the stabilizer bar and the torsional rigidity in the vehicle dynamics is carried out with the aim of finding comfort and safety of passengers. Numerical simulations show that the stabilizer bar has influence on the dynamics of the vehicle and ignore it in the mathematical model can affect the results in the suspension control projects.*

Keywords: *Vehicle dynamics, Stabilizer bar, Full-car, Nonlinear dynamics.*

1. INTRODUCTION

To improve the ride quality, adding to the comfort of the passengers, the vibrations of a vehicle body should be reduced. In recent years, much attention has been given to design control techniques of the vehicle suspension systems in order to reduce the vibrations (Liu et al., 2008; Silva et al., 2013; Tusset et al., 2014). Three types of vibration control methods have been proposed and implemented successfully, namely, the passive, the active and the semi-active method for control suspension systems (Sun et al., 2005). However the mathematical models that represent the vehicle systems in the literature are usually based on models that do not take into account the stabilizer bar related to the vertical dynamics. On the other hand, the main studies on the stabilizer bar are connected to fatigue and the vehicle dynamics in curves. This paper proposes and analysis the introduction of a stabilizing bar in a full-car model with nonlinear suspension. The analysis of the influence of the addition of the stabilizer bar and the torsional rigidity in the vehicle dynamics is carried with the aim of exploring comfort and safety of passengers.

The addition of the stabilizer bar in a full car model can be seen in figure 1.

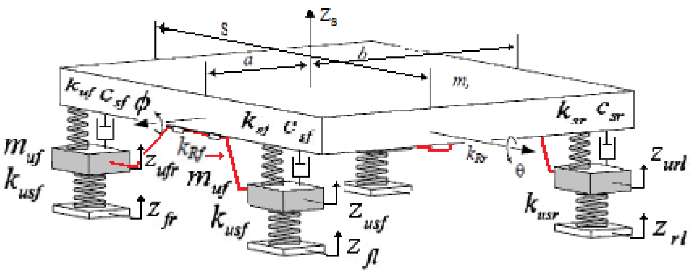

Figure 1. Full car model with stabilizer bar

Figure 1 shows the nonlinear full-vehicle model used in this work: the vehicle body is represented by a seven degree-of-freedom rigid body with mass m_s. The heave, pitch and roll motions of the sprung mass are considered. The four unsprung masses (front-left, front-right, rear-left and rear-right) are connected to each corner of the rigid body and by a stabilizing bar. A stabilizer bar is modeled as a torsional spring, the suspensions between the sprung mass and unsprung masses are modeled as nonlinear springs and nonlinear dampers elements, while the tires as modeled as linear springs.

2. MATEMATICAL MODEL

The nonlinear spring forces of front and rear suspensions are given by (Gaspar *et al*., 2003):

$$Fs_{nm} = K^{l}_{nm} u_{nm} + K^{nl}_{nm} (u_{nm})^3 \tag{1}$$

where K^{l}_{nm} is the linear coefficient stiffness, K^{nl}_{nm} is the nonlinear coefficient stiffness, u_{nm} is the deformation of the spring, and (n = front or rear, m=right or left).
The nonlinear damping forces of front and rear suspensions are given by (Gaspar *et al.*, 2003):

$$Fc_{nm} = C^{l}_{nm} \dot{u}_{nm} - C^{y}_{nm} |\dot{u}_{nm}| + C^{nl}_{nm} \sqrt{|\dot{u}_{nm}|}\ \mathrm{sgn}(\dot{u}_{nm}) \tag{2}$$

where $\dot{u}_{nm}$ is the relative velocity between the extremes of the damper, C^{l}_{nm} is the coefficient that determines the effects of the linear damper force while C^{nl}_{nm} has nonlinear impact on the damping characteristics, C^{y}_{nm} describes the asymmetric behavior of the characteristic and $\mathrm{sgn}(\dot{u}_{nm})$ is the signal function.
The tire stiffness can be considered as a linear spring, so the tire force is:

$$Ft_{nm} = K^{t}_{nm} v_{nm} \tag{3}$$

where v_{nm} is the deformation of the tire and K^{t}_{nm} is the linear coefficient stiffness.
The stabilizer bar works with the movement of the wheels is given by equation (4) (Jazer, 2008). Equation (4) relates the angle of the body and the relative displacements of the unsprung masses. Thus, when the car passes through an irregularity in only one wheel, influence occurs in the stabilizer bar and consequently in the body structure.

$$M = -K_t \left(\varphi - \frac{Z_l - Z_r}{s} \right) \tag{4}$$

Considering the vertical force, pitching force and roll force acting on sprung mass, moreover the force acting on unsprung masses, and using the nonlinear characteristics of springs and dampers, the force balance equations acting on suspension, and the accelerations are formalized in the following.

Sprung mass:

$$\begin{aligned}
\ddot{Z}_s &= \left(\frac{1}{m_s}\right)\left(-Fs_{fl} - Fc_{fl} - Fs_{fr} - Fc_{fr} - Fs_{rl} - Fc_{rl} - Fs_{rr} - Fc_{rr}\right) \\
\ddot{\phi} &= \left(\frac{1}{I_\phi}\right)\left(\frac{s}{2}\cos(\phi)\right)\left(-Fs_{fl} - Fc_{fl} + Fs_{fr} + Fc_{fr} - Fs_{rl} - Fc_{rl} + Fs_{rr} + Fc_{rr}\right) + \frac{M}{I_\phi} \\
\ddot{\theta} &= \left(\frac{1}{I_\theta}\right)\left(a\cos(\theta)\left(Fs_{fl} + Fc_{fl} + Fs_{fr} + Fc_{fr}\right) - b\cos(\theta)\left(Fs_{rl} - Fc_{rl} + Fs_{rr} + Fc_{rr}\right)\right)
\end{aligned} \tag{5}$$

Front unsprung masses:

$$\ddot{Z}_{ufl} = \left(\frac{1}{m_{uf}}\right)\left(Fs_{fl} + Fc_{fl} - Ft_{fl} - \frac{M}{s}\right)$$
$$\ddot{Z}_{ufr} = \left(\frac{1}{m_{uf}}\right)\left(Fs_{fr} + Fc_{fr} - Ft_{fr} + \frac{M}{s}\right) \tag{6}$$

Rear unsprung masses:

$$\ddot{Z}_{url} = \left(\frac{1}{m_{ur}}\right)\left(Fs_{rl} + Fc_{rl} - Ft_{rl}\right)$$
$$\ddot{Z}_{urr} = \left(\frac{1}{m_{ur}}\right)\left(Fs_{rr} + Fc_{rr} - Ft_{rr}\right) \tag{7}$$

where: m_s represents the sprung mass, I_ϕ is the roll axis moment of inertia, I_θ is the pitch axis moment of inertia, m_{unm} is the front and rear unsprung mass, K_{nm}^{l} and K_{nm}^{nl} are the front and rear suspension spring stiffness, C_{nm}^{l}, C_{nm}^{nl} and C_{nm}^{y} is the front and rear suspension damping coefficient, K_{nm}^{t} is the tire spring stiffness, a is the length between the front of vehicle and the center of gravity of sprung mass, b is the length between the rear of vehicle and the center of gravity of sprung mass and s is the width of sprung mass.

Considering the following control parameter:

$$\sigma = \frac{K_t}{K_f s^2} \tag{8}$$

where K_t is the torsional rigidity coefficient of the stabilizer bar Eq. (4), K_f represents the coefficient of linear stiffness equivalent to Eq. (1), and substituting the Eq. (8) into Eq. (4) , we find the moment of the bar

$$M = -\sigma K_f s^2\left(\varphi - \frac{y_l - y_r}{s}\right) \tag{9}$$

3. SIMULATION RESULTS

Defining the road profile as a square wave excitation given by the Eq. (10):

$$z_{fl} = h\,\mathrm{sgn}\sin(2\pi ft)$$
$$z_{fr} = h\,\mathrm{sgn}\sin(2\pi ft + \alpha)$$
$$z_{rl} = h\,\mathrm{sgn}\sin(2\pi ft + \beta)$$
$$z_{rr} = h\,\mathrm{sgn}\sin(2\pi ft + \alpha + \beta) \tag{10}$$

For numerical simulations we used the following values of the parameters adapted: (Szászi, 2002; Ishitobi, 2006; Gaspar *et al*., 2003; Zhu and Ishitobi, 2006):

Table 1. Numerical values of the system parameters.

Sprung mass, m_s	1500 [kg]
Roll axis moment of inertia, I_ϕ	460 [kg m^2]
Pitch axis moment of inertia, I_θ	2160 [kg m^2]
Front and rear unsprung mass, m_{unm}	40 [kg]
Front and rear suspension spring stiffness, K_{nm}^{l}	23500; 23800 [N/m]

Front and rear suspension spring stiffness, K_{nm}^{nl}	2350000; 2380000 [N/m]
Front and rear suspension damping coefficient, C_{nm}^{l} ; C_{nm}^{nl} ; C_{nm}^{y}	700; 400; 200 [N/m/s]
Tire spring stiffness, K_{nm}^{t}	190000 [N/m]
Length between the front of vehicle and the center of gravity of sprung mass, **a**	1.4 [m]
Length between the rear of vehicle and the center of gravity of sprung mass, **b**	1.7 [m]
S	3 [m]
$K_f s^2$	245000 [N/m^3]
H	0.08 [m]
F	9.67 [Hz]

In figure 2 we can see the vertical chassis displacement in permanent regime, when the variation of the control parameter ($0\% \leq \sigma \leq 200\%$) is considered.

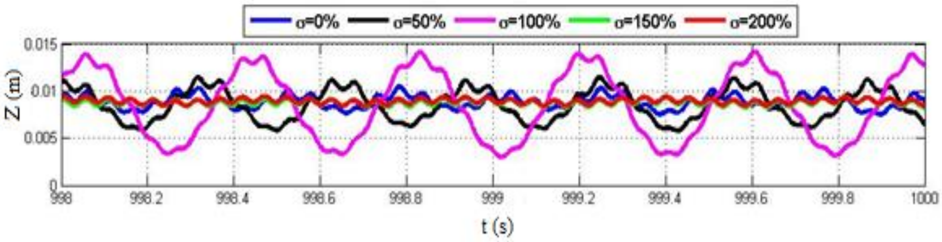

Figure 2. Vertical chassis displacement for $\alpha = 0$ and $\beta = 180^{o}$

We can observe in figure 2 that the car has good stability region without the use of stabilizer bar. The addition of the stabilizer bar to the parameter (σ≤100%) of the displacement body increases and the velocities of displacement and the angular displacement. As can be seen, when the values of σ are bigger than 100% (σ> 100%) , the stabilizer bar was effective in reduce the vertical displacement. Figure 3 shows the maximum displacement of the chassis considering the variation of the parameters (α, β and σ) in permanent regime.

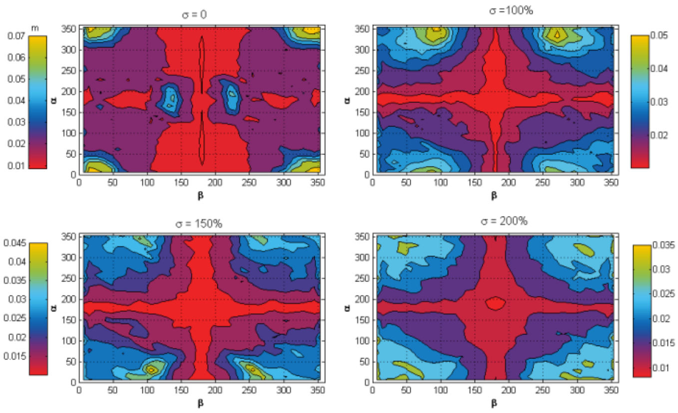

Figure 3. Levels curves of the maximum chassis displacements

It is observed that for parameter ($\alpha = 0$), there is a dependency on the angle β to reduce the vertical displacement, and with the introduction of the stabilizer bar is possible to reduce the chassis displacement.

In figure 3 we can see the maximum roll movement (ϕ) of the chassis considering the variation of parameters (α, β and σ) in permanent regime.

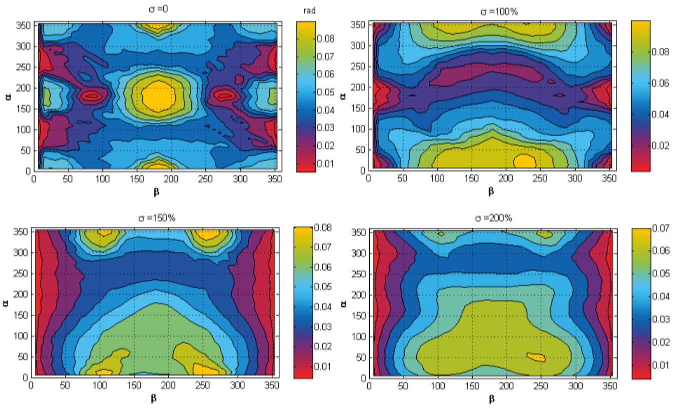

Figure 4. Levels curves of the maximum roll movement

We can observe in figure 4 that the stabilizer bar shifts the regions of higher angular displacement from the center to the extremities. It can also be viewed that occurs an increase in regions with small displacements. In figure 5 we can see the maximum displacement both vertically chassis (Z_s) as the roll movement (ϕ), considering the case where ($\alpha = 0$).

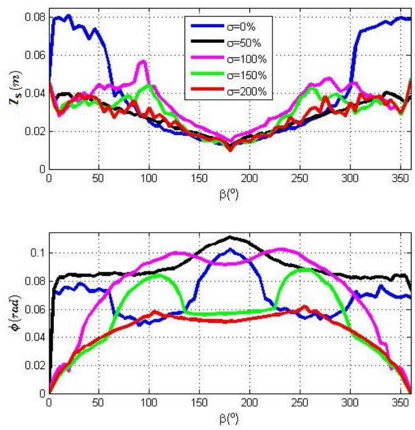

Figure 5. Influence of the angle β in the vehicle dynamics for α = 0

Figure 5 shows that the introduction of the stabilizer bar reduces the chassis displacement and decreases the maximum displacement angle of the chassis for all spectrum β. The best relationships are in ($150\% \leq \sigma \leq 200\%$).

In figure 6 we can see the maximum displacement of the wheels (Z_u) for the case of not having chassis stabilizer bar with ($\sigma = 0$) and variation of the parameters α and β.

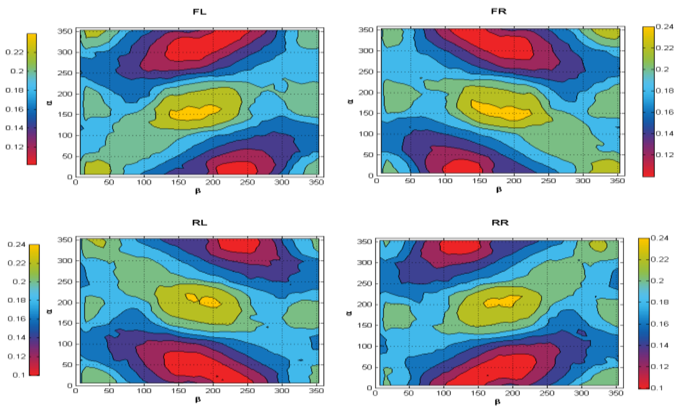

Figure 6. Maximum displacements of wheels $\sigma = 0$

It is possible to note that there is a similarity between the wheels. You can also note that in the region close to $\alpha = \beta = 180^0$ have a large displacement of the wheels region, which can cause instability of the vehicle. Figure 7 shows the maximum displacement of the wheels (Z_u) in case the frame has stabilizer bar with ($\sigma = 100\%$) and variation of the parameters α and β.

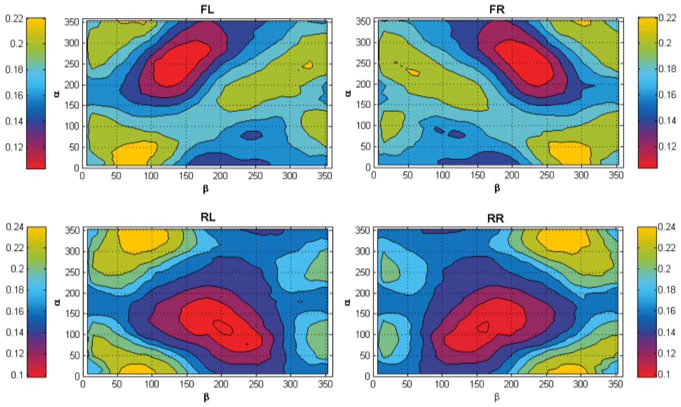

Figure 7. Maximum displacements of wheels $\sigma = 100\%$

We can see that there is a reduction of displacement and, therefore, there is an increasing to vehicle stability. In figure 8 we can see that the maximum displacement of the wheels (Z_u) when exists a stabilizer bar with ($\sigma = 150\%$) and variation of parameters α and β.

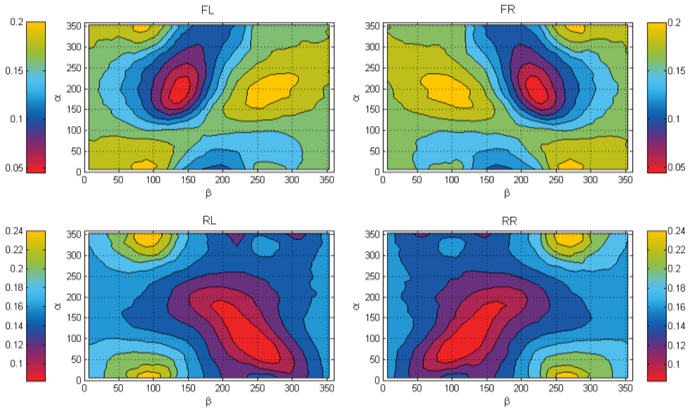

Figure 8. Maximum displacements of wheels $\sigma = 150\%$

We can observe that in figure 8, that in general there is a reduction in the front and rear wheel displacements. In figure 9 we can see the maximum displacements of the wheels (Z_u) in case the frame has stabilizer bar with ($\sigma = 200\%$) and variation of the parameters α and β.

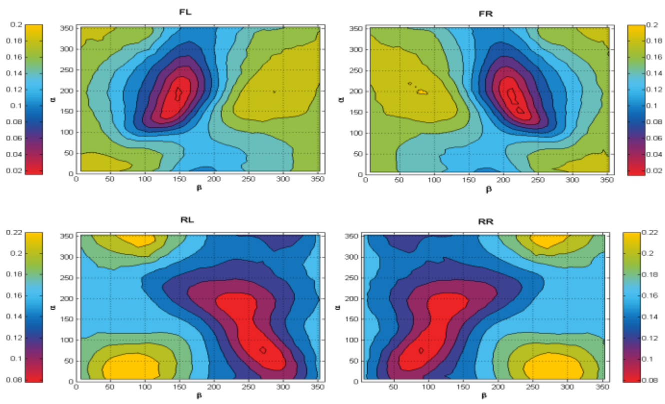

Figure 9. Maximum displacements of wheels $\sigma = 200\%$

We can observe in figure 9 an increase of the low-dislocations regions wheels in relation to Figures 6-8. Can also be seen that the introduction of the stabilizer bar produces antagonistic regions on wheels. Where the left wheel shows large displacements the right wheel presents lower amplitudes. In figure 10, we can see the influence of the parameter β on the displacements of the wheels in case the parameter α = 0.

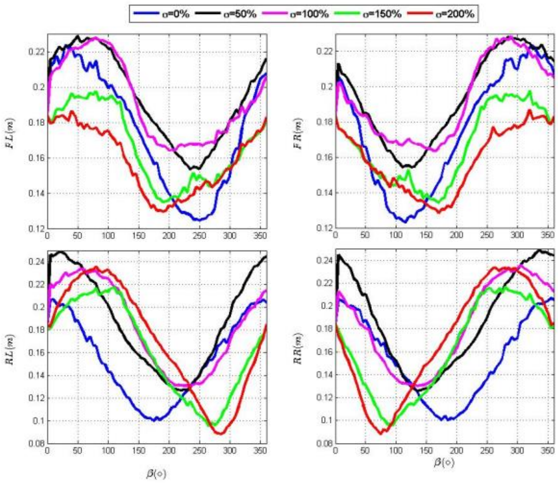

Figure 10. Influence parameter (β) on displacements of the wheels

In figure 10 we can see that the behavior of the maximum displacements of the wheels is symmetrical, and that there are points where the wheels with stabilizer bar have larger displacements than without stabilizer bar. In figure 11 we can observe the highest levels of acceleration of the chassis ($\ddot{Z}_s$) at rms (root mean square) varying the parameters α and β.

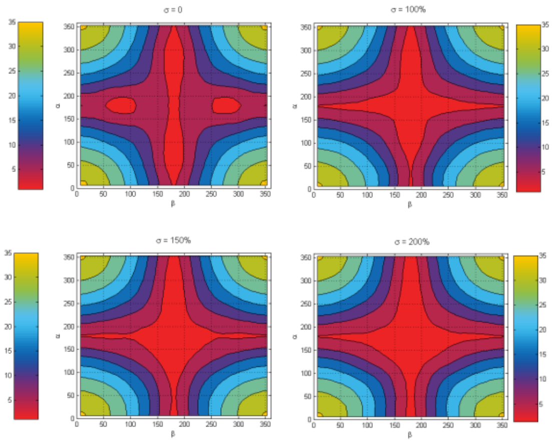

Figure 11. Níveis máximos de aceleração no chassi ($\ddot{Z}_s$)

As can be seen in figure 11 with the introduction of the stabilizer bar the acceleration level on the chassis were reduced, which generates passenger comfort to the passengers.

Comparing the previous results, we note that the same regions of smaller displacement are also the regions with less acceleration.

4. ACKNOWLEDGEMENTS

The authors thank CAPES, FAPESP and CNPQ (proc: 447539/2014-0).

5. CONCLUSIONS

We can see through numerical simulations that the use of the stabilizer bar provides an increase of the vehicle stability considering the square wave excitation, even in cases of totally alternate excitations on wheels (α and β variations). This effect is felt in the vertical chassis displacement and movement of roll to better distribute the energy.

By reducing the roll movement and vertical displacement, the stabilizer bar transfers power to the wheels and thus decreases instability conditions, enabling it that there is always a wheel with ground contact, ensuring the drivability of the vehicle.

We can also observe that the addition of the stabilizer bar provides an increased comfort level for passengers by reducing the acceleration of the chassis.

6. REFERENCES

Gaspar, P., Sazaszi, I., and Bokor, J., 2003. “Active suspension design using linear parameter varying control”. *International Journal of Vehicle Autonomous Systems*, Vol. 1, No. 2, p. 206-221.

Ishitobi, M. and Zhu, Q. 2006. “Chaotic vibration of a nonlinear full-vehicle model”. *International Journal of Solids and Structures*, n.43, p.747-759.

Liu, H., Nonami, K. and Hagiwara, T., 2008. “Active following fuzzy output feedback sliding mode control of real-vehicle semi-active suspensions”. *Journal of Sound and Vibration*, Vol. 314, p. 39-52.

Silva, R. N. E., Lenz, W. B., Balthazar, J. M., Bueno, A. M. and Tusset, A. M., 2013. “Fuzzy control strategy of a nonlinear full-car model using a magnethorheological (MR) damper”. *In: COBEM 2013, 2013, Ribeirão Preto. 22nd International Congress of Mechanical Engineering, 2013*. p. 2068-2079.

Sun, T., Huang, Z. and Chen, D., 2005. “Signal frequency-based semi-active fuzzy control for two-stage vibration isolation system”. *Journal of Sound and Vibration*, Vol. 280, p. 965-981.

Szászi, I., Gáspár, P. and Bokor, J., 2002. “Nonlinear active suspension modeling using linear parameter vary-ing approach”. *In Proceedings of the 10th IEEE Mediterranean Conference on Control and Automation*. Lisbon, Potugal.

Tusset, A. M., Piccirillo, V., Janzen, F. C., Lenz, W. B., Lima, J. J., Balthazar, J. M. and Brasil, M. R. L. F., 2014. “Suppression of vibrations in a nonlinear half-car model using a magneto-rheological damper”. *Mathematics in Engineering, Science and Aerospace: the transdisciplinary international journal*, v. 5, p. 427-443.

Zhu, Q. and Ishitobi, M., 2006. “Chaotic vibration of a nonlinear full-vehicle model”. *International Journal of Solids and Structures*, Vol. 43, p. 747-759.

7. RESPONSIBILITY NOTICE

The authors are the only responsible for the printed material included in this paper.